Received: 27 August 2020 | Revised: 16 November 2020 | Accepted: 18 November 2020

DOI: 10.1002/jcp.30190

RESEARCH ARTICLE

Journal of Cellular Physiology WILEY

Ca^{2+}-regulated cell migration revealed by optogenetically engineered Ca^{2+} oscillations

Yi-Shyun Lai[1] | Ya-Han Chang[1] | Yong-Yi Chen[1] | Jixuan Xu[1] | Chi-Sian Yu[1] | Su-Jing Chang[1] | Pai-Sheng Chen[2] | Shaw-Jenq Tsai[3] | Wen-Tai Chiu[1,4]

[1]Department of Biomedical Engineering, National Cheng Kung University, Tainan, Taiwan

[2]Department of Medical Laboratory Science and Biotechnology, National Cheng Kung University, Tainan, Taiwan

[3]Department of Physiology, National Cheng Kung University, Tainan, Taiwan

[4]Medical Device Innovation Center, National Cheng Kung University, Tainan, Taiwan

Correspondence

Wen-Tai Chiu, Department of Biomedical Engineering, National Cheng Kung University, Tainan 701, Taiwan.
Email: wtchiu@mail.ncku.edu.tw

Funding information

Ministry of Science and Technology, Grant/Award Numbers: 109-2320-B-006-037, 109-2628-B-006-012

Abstract

The ability of a single Ca^{2+} ion to play an important role in cell biology is highlighted by the need for cells to form Ca^{2+} signals in the dimensions of space, time, and amplitude. Thus, spatial and temporal changes in intracellular Ca^{2+} concentration are important for determining cell fate. Optogenetic technology has been developed to provide more precise and targeted stimulation of cells. Here, U2OS cells over-expressing Ca^{2+} translocating channelrhodopsin (CatCh) were used to mediate Ca^{2+} influx through blue light illumination with various parameters, such as intensity, frequency, duty cycle, and duration. We identified that several Ca^{2+}-dependent transcription factors and certain kinases can be activated by specific Ca^{2+} waves. Using a wound-healing assay, we found that low-frequency Ca^{2+} oscillations increased cell migration through the activation of NF-κB. This study explores the regulation of cell migration by Ca^{2+} signals. Thus, we can choose optical parameters to modulate Ca^{2+} waves and achieve activation of specific signaling pathways. This novel methodology can be applied to clarify related cell-signaling mechanisms in the future.

KEYWORDS

Ca^{2+} translocating channelrhodopsin, Ca^{2+}-dependent transcription factors, cell migration, channelrhodopsin-2, optogenetics

1 | INTRODUCTION

Calcium (Ca^{2+}) is a highly versatile secondary messenger that plays an important and ubiquitous role in intracellular signaling and regulates several cellular functions, including cell proliferation, development, differentiation, migration, transcription factor activation, and apoptosis (Berchtold & Villalobo, 2014; Berridge et al., 1998; Berridge et al., 2003). To coordinate these functions, Ca^{2+} signaling is strictly and accurately regulated and distinguished by several patterns of different spatio-temporal parameters, including amplitude, frequency, and duration (Berridge et al., 1998; Boulware & Marchant, 2008; Li et al., 1998). Spatial and temporal changes in intracellular Ca^{2+} concentration are important for determining cell fate. Recent studies have shown that Ca^{2+} signaling is highly activated in various cancers and is associated with cancer development and progression (Chen et al., 2013; Fiorio Pla et al., 2016; Xie et al., 2016). The intracellular Ca^{2+} oscillating wave can present different modes of frequency, amplitude, duty cycle, and duration. Interpretation of the messages and meanings transmitted by different Ca^{2+} oscillatory waves is critical for cellular functions.

Ca^{2+} binding domains have been identified in many molecules that are directly controlled by Ca^{2+}. Thus, the effects of Ca^{2+} patterns depend on the number of Ca^{2+} binding domains in each protein

and their affinity for Ca^{2+}. Previous studies have found that Ca^{2+} oscillating waves mainly function at different frequencies or amplitudes, and different cells and molecules respond differently to different Ca^{2+} message modes (Colella et al., 2008; Hannanta-Anan & Chow, 2016; Smedler & Uhlén, 2014), through a process called frequency decoding or amplitude decoding. Different frequencies of intracellular Ca^{2+} oscillating waves seem to be the most common strategy used by cells to transmit Ca^{2+} messages under many different physiological stimuli. Therefore, different types of cells respond to different frequency ranges of Ca^{2+} oscillation waves, and this phenomenon can be found in both in vitro cultured cells and in vivo tissue cells (Smedler & Uhlén, 2014). In addition, different protein molecules or enzymes that are directly regulated by Ca^{2+} messages also respond to Ca^{2+} signal waves in different frequency ranges, which, in turn, affect their activities. Current studies have confirmed that cAMP response element binding protein (CREB), nuclear factor κ-light-chain-enhancer of activated B cell (NF-κB), mitogen-activated protein kinase, nuclear factor of activated T cells (NFATs), Ca^{2+}/calmodulin-dependent protein kinase II (CaMKII), and calpain are all regulated by different Ca^{2+} oscillation wave modes (Colella et al., 2008; Smedler & Uhlén, 2014). Previous studies have shown that Ca^{2+} oscillation waves are most commonly used to regulate gene expression, through three signaling pathways and the corresponding Ca^{2+}-dependent gene transcription factors (Feske, 2007): (1) the calcineurin signaling pathway that activates the gene transcription factor NFAT; (2) the CaMK signaling pathway that activates the gene transcription factor CREB; (3) the IKK signaling pathway that activates the gene transcription factor NF-κB. Therefore, when a specific Ca^{2+} oscillation wave mode is generated in the cytoplasm or nucleus, the expression of specific genes is regulated by activating specific transcription factors. Ca^{2+} itself or the downstream signaling pathways/binding proteins that are activated by Ca^{2+} are closely related to gene expression regulation, and the expression of up to 60-70% of genes in the human genome is regulated by Ca^{2+} messages (Feske, 2007; Mascia et al., 2012).

The precise regulation of Ca^{2+} signaling is very important for cells to maintain life and functions. A simple Ca^{2+} ion can play a multi-faceted and important regulatory role, mainly because each Ca^{2+} wave has different concentrations, frequencies, durations, and spatial distributions within the cell and undergoes a combination of changes (Berridge et al., 2000; Hajnoczky et al., 2000). Therefore, the pattern of Ca^{2+} oscillations will be reflected in the signal transduction pathways it regulates and the physiological functions and behavioral responses of the cells. The traditional methods for stimulating physiological responses and signal transduction in cells have the disadvantage of being unable to precisely regulate specific regions in space and time within specific cells. Thus, they often cannot simulate the specific stimuli-induced reactions and effects that cells actually face.

Optogenetics is a well-established, recently developed technology for controlling the activation of cellular signaling. It combines the advantages of optics and genetics and has high precision in time and space. The specific photoreceptor protein that is translated by the optogenetic gene can respond to a specific wavelength of light, which results in a change in the three-dimensional conformation of the protein that allows regulation of the flux of specific ions or activation of specific signaling pathways downstream of the receptor (Fenno et al., 2011). This technology has been widely used in related research and applications in the fields of neuroscience, neurodegenerative diseases, and behavior, and has been successfully tested in experimental animals (Bass et al., 2010; Tsai et al., 2009). Therefore, by regulating the energy, frequency, activation time pattern, and the site of light illumination, a particular signal pattern of specific ions can be generated within a specific time and space (Mei & Zhang, 2012). The light-sensitive and cation-selective ion channel channelrhodopsin 2 (ChR2) found on *Chlamydomonas reinhardtii* and *Volvox carteri* has been fully developed for optogenetic manipulations (Nagel et al., 2002, 2003). Its maximum absorption is within the blue light spectrum, near 470–480 nm, and it can be quickly activated when it is irradiated for 1–3 ms. However, ChR2 is conductive to both positive monovalent and divalent cations and is not a specific Ca^{2+} channel. The molecular tool used in this study project is CatCh (Ca^{2+} translocating channelrhodopsin), which is a ChR2 protein carrying a point mutation (Kleinlogel et al., 2011). CatCh responds to light 70 times faster and is six times more permeable to Ca^{2+} compared to wild-type ChR2. Therefore, it is very suitable for use as an optogenetic Ca^{2+} research tool. This study aimed to clearly, accurately, and instantly elucidate the regulation of cell migration by Ca^{2+} signals.

2 | MATERIALS AND METHODS

2.1 | Cell culture and chemical reagents

The human bone osteosarcoma cell line U2OS was maintained in low-glucose Dulbecco's modified Eagle's medium (DMEM; Gibco) supplemented with 10% fetal bovine serum (FBS; Gibco), penicillin (100 IU/ml), and streptomycin (100 μg/ml) in 5% CO_2 at 37°C. Ionomycin was purchased from Sigma-Aldrich. Celastrol was purchased from Toronto Research Chemicals. LY294002 and Wortmannin were purchased from Cayman Chemical.

2.2 | DNA transfection

U2OS cells were transfected with enhanced green fluorescent protein (EGFP)-tagged ChR2 and NFAT, Venus-tagged CatCh, and RFP-tagged NFAT, NF-κB, and CREB plasmids using Lipofectamine 3000 (Invitrogen) and used for experiments 48 h later. Stable clones were selected using 500 μg/ml geneticin (G418; Gibco) and then sorted using flow cytometry (FACSAria; BD Biosciences).

2.3 | Wound-healing assay

The ibidi culture-inserts 2 well (ibidi) were applied to assess U2OS cell migration. The insert consisted of two wells separated by a

500-μm-thick silicon wall. U2OS cells were seeded at an equal density (2×10^4 cells in 100 μl) in culture medium containing 10% FBS and incubated at 37°C in 5% CO_2 overnight. The insert was removed after the cells were well attached and formed a monolayer; then, cells were incubated with or without different inhibitors in DMEM containing 10% FBS. At the same time, blue light illumination, with different parameters, was given to the cells. Cell migration into the gap (initially ~500 μm) was recorded every 24 h via phase-contrast microscopy. The data were collected from three independent experiments and analyzed as wound closure (%) using ImageJ software (NIH).

2.4 | Optogenetic platform

A LED illumination system (Thorlabs) supplied a 470 nm blue light, and DC2100 software connected to a function generator was used to manipulate the optical parameters (power, frequency, duty cycle, and duration) and illuminate cells with blue light. According to the experimental requirements, a single 470 nm LED light source could be operated under a microscope to detect fluorescent changes in real time after blue light illumination of the cells. Moreover, a customized 470 nm LED array light box consisted 42 high power (1 W) LED bulbs was used, and a power meter device (OPHIR NOVA II, Jerusalem, Israel) measured the LED light output power.

2.5 | Single-cell intracellular Ca^{2+} measurements

The changes in fluorescence intensity related to intracellular Ca^{2+} levels in living U2OS cells were measured using a single-cell fluorimeter (Till Photonics). The fluorescent protein-based Ca^{2+} indicator R-GECO (red fluorescent, genetically encoded Ca^{2+} indicator for optical imaging) was used as an intracellular Ca^{2+} probe with excitation at 560 nm wavelength. R-GECO was transfected into CatCh-Venus overexpressing U2OS cells before blue light illumination. The fluorescence emission intensity was monitored at 590 nm, stored digitally, and analyzed using the software TILLvisION 4.0 (Till Photonics, Grafelfing, Germany).

2.6 | Time-lapse recording

The time-lapse images of nuclear translocation of transcription factors (NFAT, NF-κB, and CREB) were recorded using an inverted wide-field fluorescence microscope (Olympus IX71). Cells overexpressing fluorescent protein-tagged transcription factors (NFAT, NF-κB or CREB) and CatCh-Venus were cultured at a density of 5×10^4 cells/3 cm in glass-bottomed dishes and kept in phenol red-free medium inside a mini-incubator at 37°C with moderate humidity. Live cell images of transcription factors were recorded every 5 min continuously, for 25 min, under blue light illumination.

2.7 | Live-dead assay

For cell viability analysis, 5×10^4 U2OS cells were seeded in 3-cm dishes and grown overnight as a monolayer. Then, the cells were illuminated with 470 nm blue light illumination with different parameters. Each group of cells was washed with DMEM medium and stained with 2 μg/ml Hoechst 33342 (nucleus), 1 μM calcein AM (live cells), and 1 μM ethdium-1 (dead cells) post illumination. Next, fluorescent images were taken using microscopy, and cell viability was analyzed with ImageJ software (NIH).

2.8 | Western blot analysis

Cell lysates were harvested in radioimmune precipitation assay buffer containing 150 mM NaCl, 10 mM EDTA, 50 mM Tris-HCl at pH 7.4, 1% NP-40, 0.004% sodium azide, 0.5% sodium deoxycholate, 0.1% SDS, and protease inhibitor cocktail (Roche cOmplete™), which was supplemented with 1 mM NaF, 1 mM phenylmethylsulfonyl fluoride, and 1 mM Na_3VO_4. Whole cell lysate proteins were separated by SDS-PAGE and electroblotted onto nitrocellulose membranes, which were incubated with several primary antibodies, including NFAT, phospho-CREB (Abcam), phospho-NF-κB, NF-κB, CREB, phospho-Stat3, Stat3, phospho-AKT, AKT, phospho-p38, p38, phospho-ERK, ERK (Cell Signaling), phospho-JNK, JNK (Santa Cruz), and β-actin (Sigma-Aldrich). The immunocomplexes were then detected with horseradish peroxidase-conjugated IgG (Jackson ImmunoResearch Laboratories), and the reaction was developed using an ECL detection kit (Amersham) in an ImageQuant LAS 4000 system (GE Healthcare Life Sciences).

2.9 | Statistical analysis

All data are reported as mean ± *SEM*. The Student's *t*-test or one-way analysis of variance with Dunnett's post-hoc test was used to assess the statistically significant differences between groups. A $p < .05$ was considered statistically significant.

3 | RESULTS

3.1 | Establishment of an optogenetically engineered Ca^{2+} oscillation platform

The signal generator and light source controller were used to control and edit the output intensity (mW/mm^2), frequency (Hz), duty cycle, and duration of each illumination generated by high-power LED or laser at 470 nm. ChR2-EGFP and CatCh-Venus DNA constructs were stably expressed in the human osteosarcoma cancer U2OS cell line, to generate optogenetically engineered Ca^{2+} oscillations. Both ChR2 and CatCh expression in the plasma membrane were confirmed by immunostaining and confocal microscopy (Figure 1a). The changes in

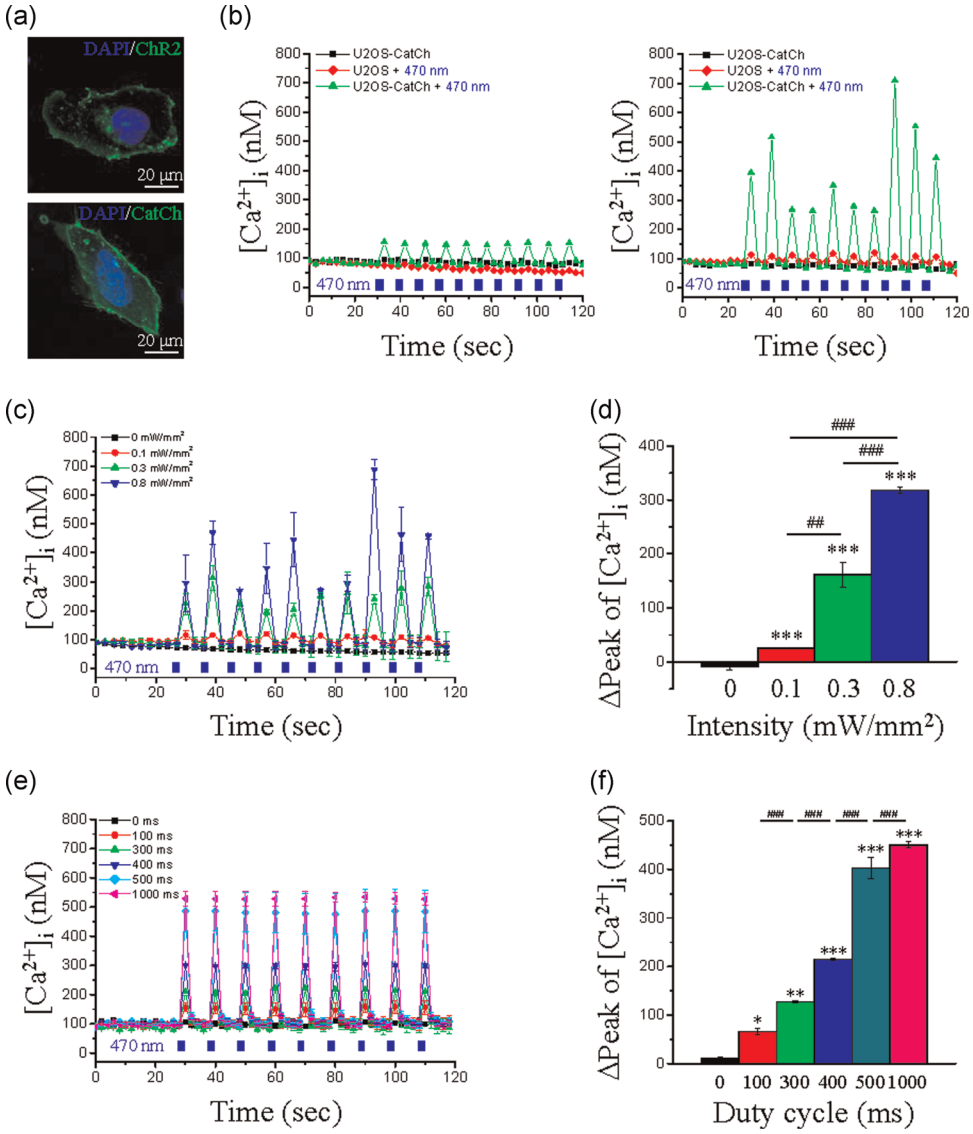

FIGURE 1 Ca^{2+} oscillations can be triggered by different illumination modes. (a) Confocal images of ChR2-EGFP and CatCh-Venus stable expression in U2OS cells. Scale bar = 20 μm. (b) The changes in intracellular Ca^{2+} ($[Ca^{2+}]_i$) are represented by R-GECO emission light intensity. R-GECO plasmids were transfected and expressed in U2OS cells overexpressing ChR2-EGFP or CatCh-Venus. ChR2 or CatCh was excited with a blue laser at a wavelength of 470 nm (the blue squares in the picture), and R-GECO was excited with a 543 nm laser using a confocal microscope for Ca^{2+} recording. (c) U2OS cells overexpressing CatCh-Venus were either not illuminated (0 mW/mm^2) or illuminated with 470 nm blue light at 0.1, 0.3, or 0.8 mW/mm^2 with 0.1 Hz fixed light frequency, 1 s duty cycle, and 2 min activation time. (d) Analysis of the maximum change in the increase of $[Ca^{2+}]_i$ (ΔPeak of $[Ca^{2+}]_i$). (e) U2OS cells overexpressing CatCh-Venus were either not illuminated (0 ms) or given 100, 300, 400, 500, or 1000 s illumination duty cycles under 0.8 mW/mm^2 fixed light intensity, 0.1 Hz light frequency, and 2-min activation time, throughout the experiment. (f) Analysis of the maximum change in the increase of $[Ca^{2+}]_i$ (ΔPeak of $[Ca^{2+}]_i$). $^{*}p < .05$; $^{**,\#\#}p < .01$; $^{***,\#\#\#}p < .001$, calculated were using a one-way analysis of variance

intracellular Ca^{2+} concentrations were represented by the emission light intensity of the fluorescent protein-based Ca^{2+} indicator R-GECO. The results showed no significant changes in intracellular Ca^{2+} concentrations ($[Ca^{2+}]_i$) in cells that expressed ChR2 or CatCh and were not given blue light illumination (U2OS-ChR2, U2OS-CatCh), nor in wild-type cells that did not express ChR2 or CatCh but were given blue light illumination (U2OS + 470 nm). In contrast, oscillations that reflected an increase in $[Ca^{2+}]_i$ were recorded when cells expressing ChR2 or CatCh were illuminated with blue light (U2OS-ChR2 + 470 nm, U2OS-CatCh + 470 nm) (Figure 1b). Our results showed that both ChR2 or CatCh could be activated and generate Ca^{2+} oscillations upon 470 nm blue light illumination. However, the mutated CatCh produced higher intracellular Ca^{2+} elevations than the wild-type ChR2; and thus, CatCh was more suitable for use as an optogenetic tool for Ca^{2+} research in this study.

Next, we examined whether different Ca^{2+} oscillation patterns could be generated using this optogenetic platform. The results showed that the maximum change in $[Ca^{2+}]_i$ (ΔPeak of $[Ca^{2+}]_i$) increase in the illuminated groups showed a light intensity-dependent increase (Figure 1c,d). In addition to the effects of light intensity on

Ca^{2+} oscillation, we also demonstrated a duty cycle-dependent increase of $[Ca^{2+}]_i$ (Figure 1e,f). According to these results, it was confirmed that illumination of CatCh-expressing cells with blue light of different parameters induces different Ca^{2+} patterns inside the cells.

3.2 | Manipulation of CatCh-mediated Ca^{2+}oscillations to evaluate cell viability and migration

The previous experiments demonstrated that CatCh mediates Ca^{2+} influx in the cytosol after illumination with 470 nm light. We used the live-dead assay to further examine the effects on Ca^{2+}-induced cell death, to discriminate its effect on cell migration. Calcein AM was used to distinguish live cells, whereas ethidium-1 was used as dead cell marker. Specifically, ethidium-1 enters the damaged cell membranes of dead cells and binds to nucleic acids. U2OS-CatCh cells were stimulated with four different frequencies (0.01, 0.1, 1 and 10 Hz) of blue light, for 30 and 60 min, to investigate the effects of Ca^{2+} frequency on the cell death. More than 20% of the cells were dead after stimulation by light illumination at 10 Hz for 30 min, whereas 0.01, 0.1, and 1 Hz stimulations did not induce cell death (Figure 2a,b). After 60 min of light stimulation with 10 Hz, more than 90% of the cells died. In addition, stimulation with 1 Hz light induced over 5% cell death (Figure 2c,d). To determine whether Ca^{2+} oscillations were the main factor leading to cell death, we examined the viability of U2OS-WT cells following light illuminations. The results showed no cell death after light illuminations, even at 10 Hz (Figure 3). Thus, we concluded that the light-stimulated cell death of U2OS-CatCh cells was caused by Ca^{2+} oscillations, but not by the heat and/or phototoxicity that are associated with light illuminations. We evaluated cell viability over long illumination periods, and found that illumination at 1 Hz induced 10%, 70%, and 90% cell death at 1, 3, and 6 h, respectively. In contrast, illumination at 0.01 and 0.1 Hz neither affected the number of cells nor induced cell death, even after 6 h of illumination (Figure 2e). Moreover, we also further analyzed that even after 6 or 12 h of 0.01 or 0.1 Hz light illumination, no obvious changes in cell number and cell death occurred after standing for 48 h (Figure S1). Based on these results, we decided to use the 0.01 and 0.1 Hz frequencies in subsequent experiments. We concluded that a higher frequency light illumination induces Ca^{2+} oscillations that mediate cell death. This could be due to the high amount of Ca^{2+} entering the cytosol, with toxic effects thus leading to either necrosis or apoptosis (Kass & Orrenius, 1999).

Ca^{2+} signaling plays an important role in regulating cell migration. The wound-healing assay was performed to examine the effects of Ca^{2+} oscillations produced with different frequencies of illumination on cell migration. Based on the previous experiments, we applied blue light illumination at 0.01 and 0.1 Hz frequencies, which had no effect on cell viability. The results showed that there was a difference between 0.01 and 0.1 Hz at 24 and 48 h after illumination with blue light for 6 h (Figure 4a) and 12 h (Figure 4c). We found that the cell migration during wound healing was obviously higher than that with non-light treatment at a frequency of 0.01 Hz for 6 and 12 h (Figure 4b,d). However, cell migration obviously decreased following illumination with 0.1 Hz frequency for 6 and 12 h (Figure 4b,d).

3.3 | Optogenetically engineered Ca^{2+}oscillations activate Ca^{2+}-dependent transcription factors

The execution of Ca^{2+} signaling can activate certain Ca^{2+}-dependent transcription factors by regulating the activity of various kinases and phosphatases. The activation of Ca^{2+}-dependent transcription factors, such as NFAT, NF-κB, and CREB, leads to their nuclear translocation and gene expression (Dolmetsch et al., 1997; Nankova et al., 1996; Uhlén & Fritz, 2010). To assess the influence of Ca^{2+} on the activity of these Ca^{2+}-dependent transcription factors, ionomycin was applied as a chemical stimulator in fluorescent protein RFP-tagged transcription factor overexpressing U2OS cells. Ionomycin is a Ca^{2+} ionophore that forms a channel on the plasma membrane and directly transports Ca^{2+} inside the cell (Dedkova et al., 2000). Time-lapse images showed the dynamic changes that followed ionomycin treatment (Figure 5). Before Ca^{2+} simulation, a dominant fraction of NFAT-RFP and NF-κB-RFP was present in the cytoplasm, but most of the CREB-RFP accumulated in the nucleus. After treatment with 2 μM ionomycin, NFAT-RFP and NF-κB-RFP gradually accumulated in the nucleus after about 15–20 min, and the intensity of CREB-RFP also increased in the nucleus. These results indicated that Ca^{2+}-dependent transcription factors NFAT, NF-κB, and CREB were truly activated by ionomycin-induced Ca^{2+} influx. However, the signaling mechanism underlying the effect of intensity and frequency of Ca^{2+} oscillation remained elusive. Therefore, we subsequently used optogenetics to investigate the relationship between Ca^{2+} oscillation and transcription factor activation. First, CatCh-overexpressing U2OS cells continuously illuminated with blue light, and the results showed Ca^{2+} influx. Furthermore, the channels may have exhibited switch fatigue, because the amount of Ca^{2+} gradually declined (Figure 6a). Before optogenetic simulation, a dominant fraction of NFAT-EGFP was present in the cytoplasm. However, NFAT-EGFP accumulated in the nucleus gradually, starting at 10 min, and fully localized in the nucleus at 20–25 min post blue light illumination (Figure 6b).

It is known whether the transcriptional activity of Ca^{2+}-dependent transcription factors is regulated by Ca^{2+} oscillations (Boulware et al., 2008; Dolmetsch et al., 1997; Parekh, 2011; Smedler et al., 2014; Song et al., 2012). However, how cells decode oscillatory signals with respect to amplitude, frequency, and duty cycle remains unknown. To understand how the different Ca^{2+} waves independently affects transcription, we investigated the effectiveness of transcriptional activation under different intensities and frequencies of blue light illumination. Here, phosphorylation and dephosphorylation of the transcription factors NFAT, NF-κB, and CREB were analyzed by Western blot analysis (Figure 7). Stronger light intensity and longer illumination times led to higher Ca^{2+} concentrations within the cells. We found that NFAT

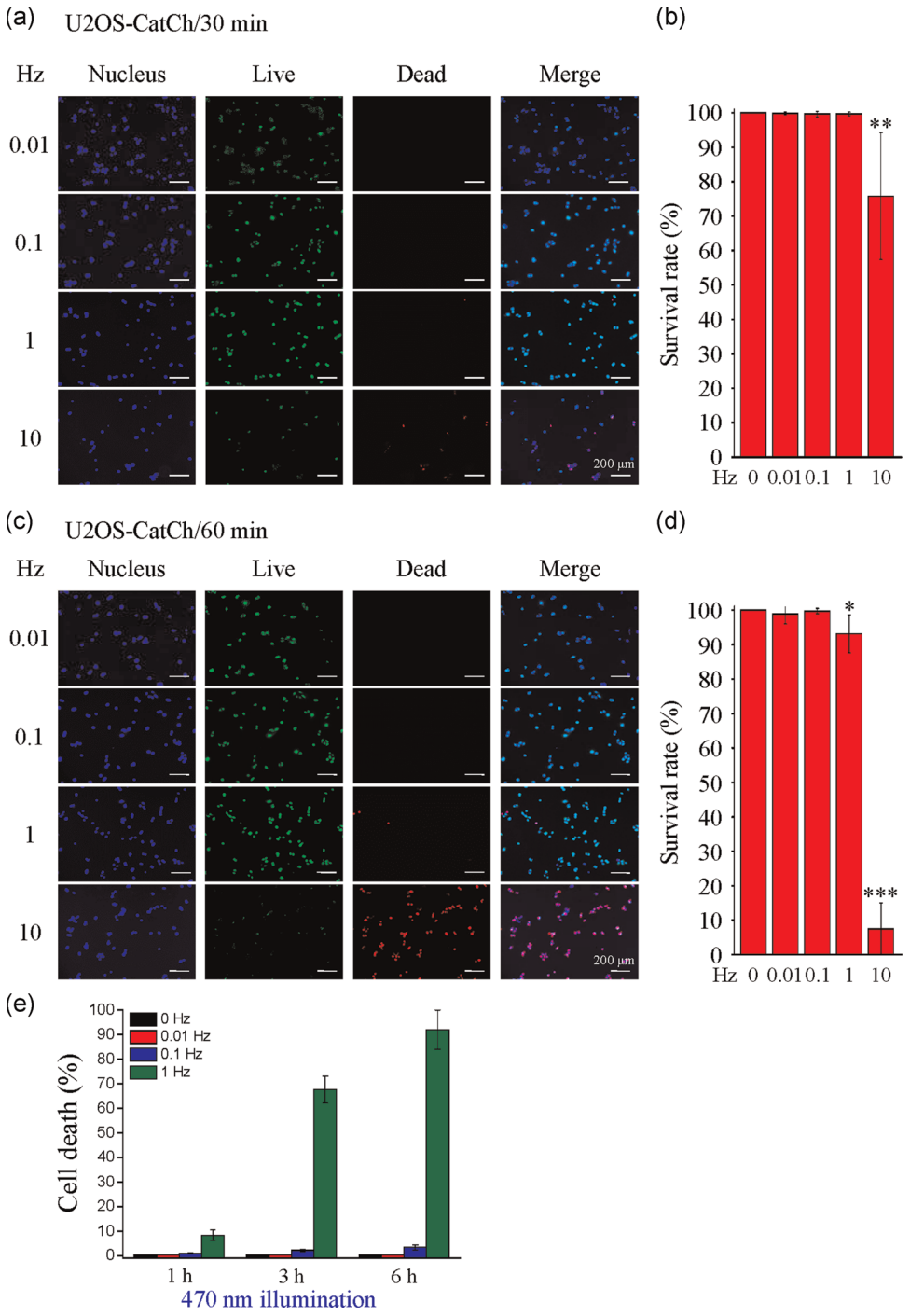

FIGURE 2 Effects of CatCh-mediated Ca^{2+} oscillations on cell survival. Live-dead analysis of U2OS cells overexpressing CatCh (U2OS-CatCh) at 48 h after light illumination. (a,c) Representative fluorescence images (nucleus: blue; live cells: green; dead cells: red) of U2OS-CatCh cells after (a) 30 or (c) 60 min of light illumination at different frequencies (0.01, 0.1, 1, and 10 Hz), fixed 0.1 mW/mm^2 power and 100 ms duty cycle. Hoechst 33,342 was used to identify nuclei. Scale bar = 200 μm. (b,d) Quantitative analysis of survival rate from (a) and (c), respectively. (e) Quantitative analysis of cell death of U2OS-CatCh cells after different periods of light illumination with different frequencies. *$p < .05$; **$p < .01$; ***$p < .001$, calculated by Student's *t*-test

was significantly activated, as dephosphorylated NFAT (de-p-NFAT) levels increased significantly under high-intensity light (0.3 mW/mm^2). The activity reached the highest level after 15 min of light illumination and then decreased after 30 min of light illumination. In addition, deactivation of NFAT, as phosphorylated NFAT (p-NFAT), was observed after 60 min of light illumination (Figure 7a). In contrast, NF-κB showed significant activation under low-intensity light (0.1 mW/mm^2), and NF-κB activity gradually

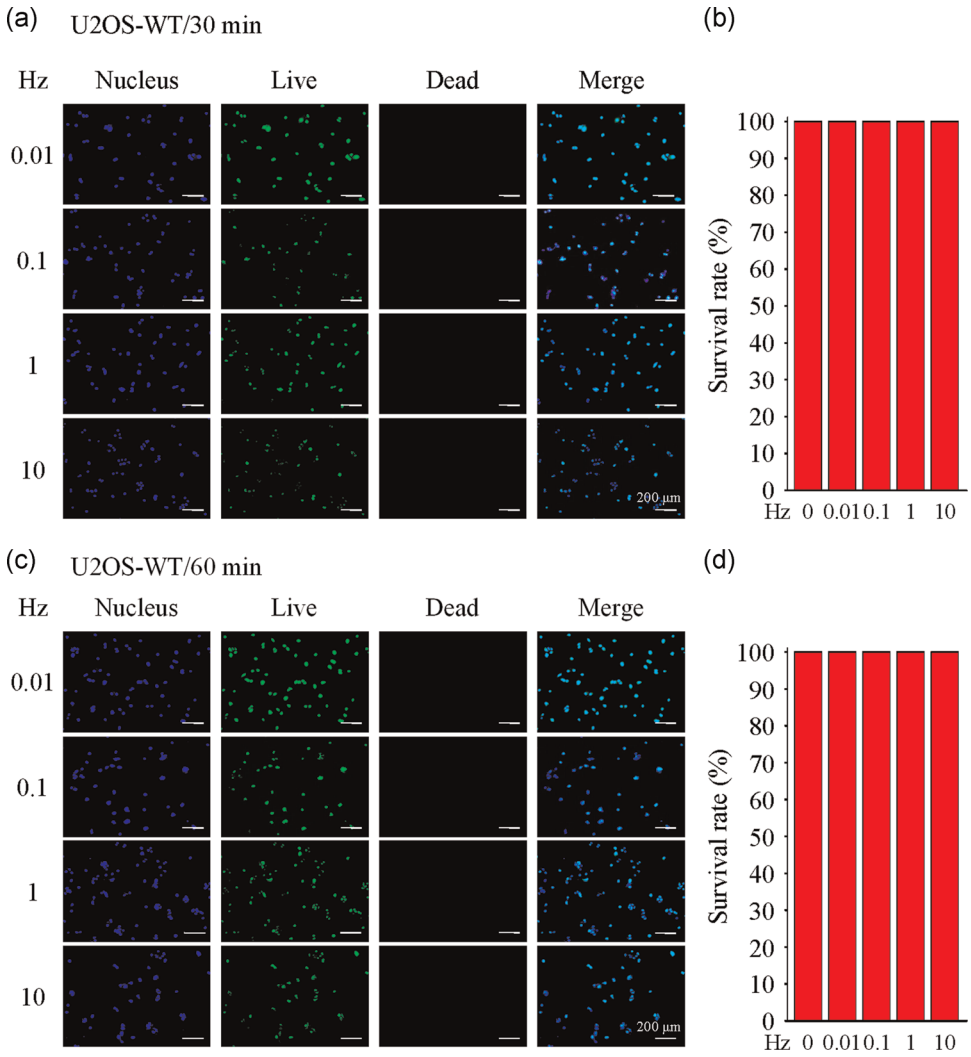

FIGURE 3 Effects of light illumination on cell survival. Live-death analysis of the parental U2OS cells (U2OS-WT) at 48 h after light illumination. (a,c) Representative fluorescence images (nucleus: blue; live cells: green; dead cells: red) of U2OS-WT cells after (a) 30 or (b) 60 min of light illumination at different frequencies (0.01, 0.1, 1, and 10 Hz), 0.1 mW/mm^2 fixed power and 100 ms duty cycle. Hoechst 33342 was used to identify nuclei. Scale bar = 200 μm. (b,d) The quantitative analysis of survival rate from (a) and (c), respectively

increased with the increase in illumination time from 15 to 60 min, but this was not observed upon illumination with high-intensity light (0.3 mW/mm^2) (Figure 7b). As shown in Figure 7c, CREB activity gradually increased, in the presence of both low-intensity light (0.1 mW/mm^2) and high-intensity light (0.3 mW/mm^2), with increasing illumination time. Furthermore, high intensity light had a greater effect on CREB activation than low intensity light (Figure 7c). The effects of Ca^{2+} frequency on the activation of these three transcription factors were similar to the changes caused by light frequency (Figure 7d–f). NFAT was significantly activated, as dephosphorylated NFAT (de-p-NFAT), only under high frequency light (1 Hz) after 60 min of illumination (Figure 7d). In contrast, NF-κB presented significant activation under low frequency light (0.01 Hz), after 30 and 60 min of illumination (Figure 7e). Lastly, CREB activation was observed under low frequency light (0.01 Hz) and high frequency light (1 Hz) illumination (Figure 7f).

3.4 | Activation of NF-κB through CatCh-mediated Ca^{2+} oscillations enhances cell migration

Our results showed that illumination with 0.01 Hz did not induce cell death, even over a long illumination period (Figure 2e,s1), and cell migration was enhanced at a frequency of 0.01 Hz (Figure 4). In addition, we found that NF-κB could be activated by a lower concentration of Ca^{2+} (Figure 7b,e). Here, we investigated the signaling pathways involved in promoting cell migration. In this experiment, the cell migration speed of the dimethyl sulfoxide control group increased under light illumination. Using the NF-κB inhibitor Celastrol we found that the cell migration speed decreased at 24 h, compared to cells that were not pretreated with the inhibitor (Figure 8). The inhibition of NF-κB by celastrol was confirmed by Western blot analysis (Figure 2).

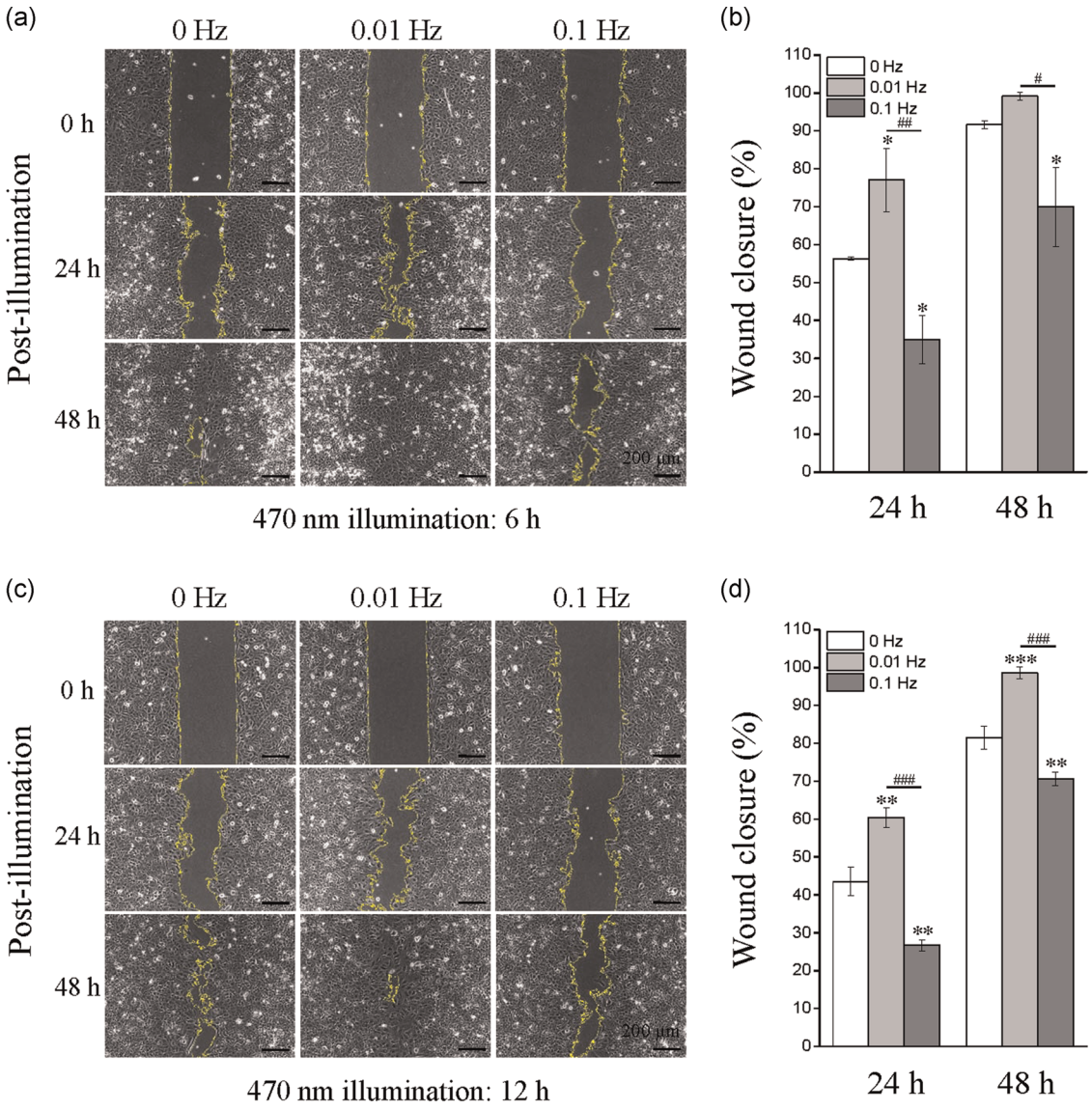

FIGURE 4 Modulation of Ca^{2+} oscillations by low frequencies enhances cell migration. In vitro wound healing migration assay was performed to evaluate the effect of light illumination on cell migration. U2OS-CatCh cells were seeded into silicon inserts containing 10% fetal bovine serum medium. Following cell adhesion, inserts were removed, and the cells were incubated for 48 h. Phase images were captured every 24 h and wound spaces were analyzed using ImageJ. (a,c) After insert removal, cells were illuminated with 470 nm blue light at different illumination frequencies (0.01 and 0.1 Hz) under a fixed light power (0.1 mW/mm^2), duty cycle (100 ms), and (a) 6 h or (c) 12 h of light illumination. (b,d) Cell migration is presented as the percentage of wound closure. Each bar represents the mean ± *SEM* from three independent experiments. *Significant difference between cells treated with light illumination (0.01 and 0.1 Hz) and control nontreated cells (0 Hz). $^{*,\#}p < .05$; $^{**,\#\#}p < .01$; $^{***,\#\#\#}p < .001$, calculated by one-way analysis of variance

4 | DISCUSSION

There is a great difference in the distribution, concentration, duration, and frequency of Ca^{2+} fluctuations in specific subcellular compartments in response to different stimuli. Different Ca^{2+} signals in different cell types result in different biological behaviors. For example, a low Ca^{2+} oscillatory wave can result in sperm-egg fusion (Whitaker, 2006), while a high Ca^{2+} oscillation can lead to bone differentiation (Sun et al., 2007). At present, traditional cell signaling biomedical research has mainly relied on pharmacological and biochemical stimulation, physical stimulation (mechanical or electrical), or gene expression to examine cell physiological responses and signal transduction. However, such methods cannot take into account both spatial and temporal distribution of Ca^{2+} changes. That is, researchers cannot accurately control the time, frequency, and position of the signaling pathways that are induced by specific distribution. Thus, they can only passively observe the changes in the concentration, spatial distribution, and duration of the Ca^{2+} signal generated under the relevant stimuli and indirectly infer the role and corresponding

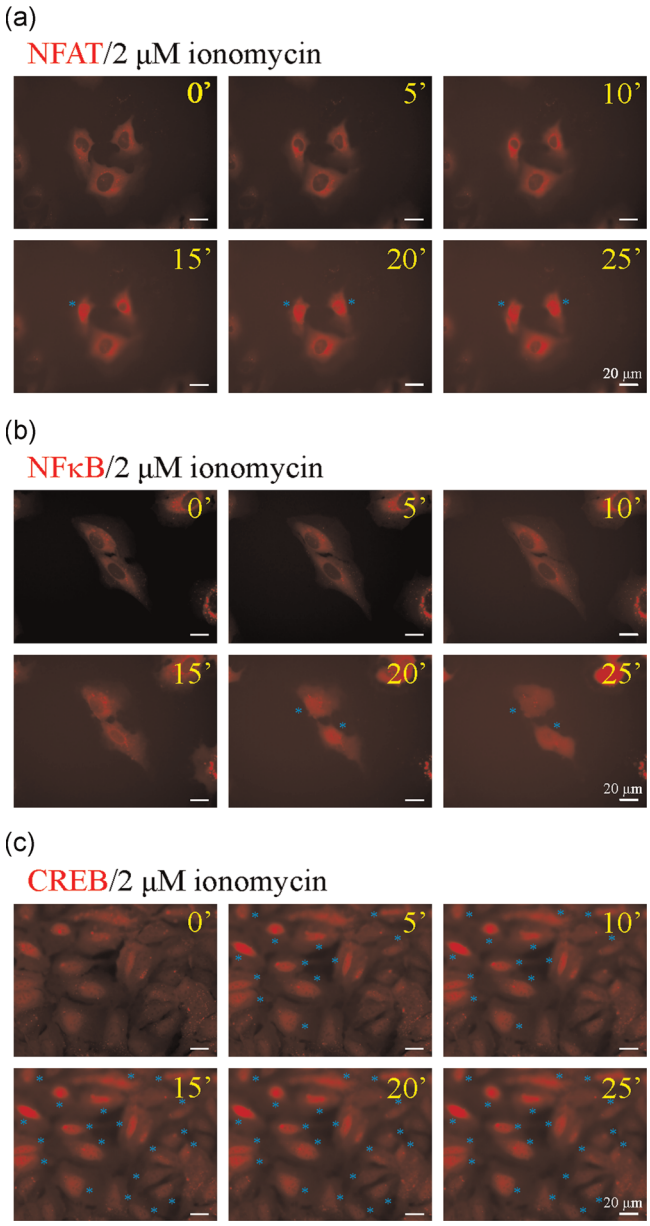

FIGURE 5 Ca^{2+} influx induces nuclear translocation of Ca^{2+}-dependent transcription factors. After overexpression of RFP-tagged (a) NFAT, (b) NF-κB, and (c) CREB in U2OS cells, cells were treated with 2 μM ionomycin for 25 min. Time-lapse imaging of RFP in living cells was performed in 5-min intervals under a wide-field microscope. Cyan stars indicate nuclear translocation of RFP-tagged transcription factors after ionomycin treatment. Scale bar = 20 μm. CREB, cAMP response element binding protein; NFAT, nuclear factor of activated T cell; NF-κB, nuclear factor κ-light-chain-enhancer of activated B cell; RFP, red fluorescent protein

function of the Ca^{2+} signal. To clarify the mechanisms of Ca^{2+} effects generated by specific physical and pharmacological stimuli, we can utilize the accuracy of light in time and space to actively generate different Ca^{2+} patterns and replace the traditional passive record of stimulated Ca^{2+} signals with optogenetically engineered Ca^{2+} oscillations.

In this study, we used the CatCh molecular optogenetic tool to create different Ca^{2+} oscillations (Figure 1), thus affecting Ca^{2+}-dependent transcription factors (Figures 6 and 7) and other signaling pathways (Figure S3). In a recent study, it was shown that transcription factor activation can be regulated by different Ca^{2+} oscillation frequencies (Hannanta-Anan et al., 2016; Smedler et al., 2014). In this study, we used optogenetics to manipulate the patterns of Ca^{2+} oscillations and thereby regulate cell migration (Figure 4). Both the intensity and frequency of light illumination can elevate intracellular Ca^{2+} levels. The activation of these Ca^{2+}-dependent transcription factors by optogenetics consistently depends on the intensity and frequency of light illumination (Figure 7). We also found that the transcription factor CREB transcription factor could be phosphorylated and activated at both low and high Ca^{2+} levels. NFAT tended to undergo dephosphorylation and activation at high Ca^{2+} levels, whereas NF-κB presented significant phosphorylation and activation at low Ca^{2+} levels (Figure 7). These findings clearly shows that activation of different Ca^{2+}-dependent transcription factors depends on different Ca^{2+} oscillation patterns, which can explain the variation of Ca^{2+} oscillation patterns and signal transduction pathways activated by different physiological stimuli. Moreover, our results showed that NFAT activation requires higher Ca^{2+} concentrations than NF-κB. This observation can be explained by the results of a previous study, which found that store-operated Ca^{2+} entry-mediated Ca^{2+} oscillations underlie NFAT regulation, which suggests that NFAT needs both ER efflux and extracellular Ca^{2+} influx (Kar et al., 2012; Ong et al., 2012). This result demonstrates that the NFAT activation threshold is higher than that of NF-κB.

Previous research has also reported the relationship between NFAT and NF-κB with regard to Ca^{2+} requirements. Dolmetsch et al. have shown that NF-κB was stimulated by a transient Ca^{2+} increase, while NFAT activation required sustained Ca^{2+} influx (Dolmetsch et al., 1997). Cell migration has also been found to rely on different Ca^{2+} concentrations (Franco & Huttenlocher, 2005; Huttenlocher et al., 1997; Ridley et al., 2003). For example, calcium ion sparklets were found to be generated in the front of the migratory cells (Kim et al., 2016; Wei et al., 2009). In addition, in polarized cells it has been observed that Ca^{2+} shows a concentration gradient from rear to front and this gradient is necessary for directional migration (Huang et al., 2015; Wei et al., 2012). Ca^{2+} influx into cells also activates Ca^{2+}-associated downstream signals, including ERK, AKT, Stat3, p38, and JNK (Huang et al., 2004; Jiehui et al., 2015; Sáez et al., 2014). In this study, we used optogenetics to generate different Ca^{2+} patterns and explore the Ca^{2+} signaling pathways that affect cell migration. We found that cells illuminated with high frequency (1 Hz) blue light for 1 h presented decreased cell migration (data not shown). After a longer illumination for 6 and 12 h, we observed a significant increase or decrease in cell migration speeds at 0.01 and 0.1 Hz illumination frequencies, respectively (Figure 4). To summarize, we found that the best parameters for increasing cell migration included 0.1 mW/mm^2 intensity, 100 ms duty cycle, and 0.01 Hz frequency. Under that illumination, we observed obvious

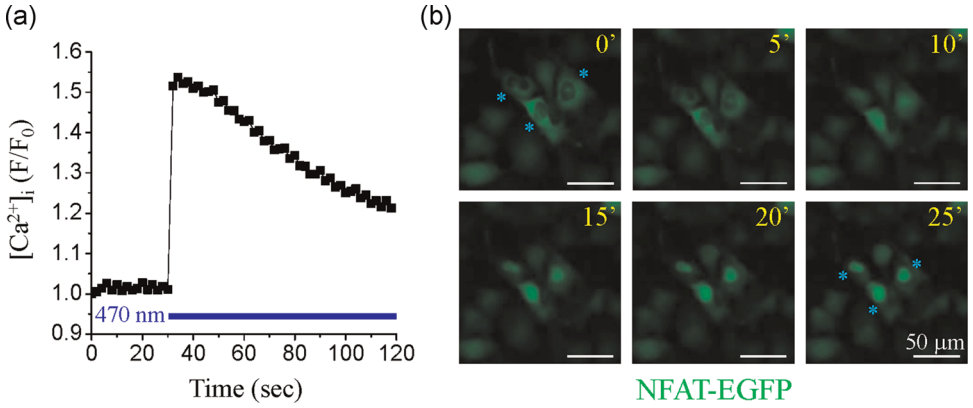

FIGURE 6 Optogenetically generated Ca^{2+} oscillations activates nuclear entry of the transcription factor NFAT. (a) CatCh-Venus and R-GECO were overexpressed in U2OS cells that were illuminated with 470 nm blue light under 0.3 mW/mm^2 fixed intensity, 1 Hz frequency, 500 ms duty cycle, and 2 min activation time throughout the experiment. The blue line in the picture represents CatCh activation by blue light. The changes in intracellular Ca^{2+} ($[Ca^{2+}]_iF/F_0$) are represented by the R-GECO emission intensity. (b) CatCh-Venus and NFAT-EGFP overexpressing U2OS cells were illuminated with 470 nm blue light as described in (a). Time-lapse imaging of EGFP in live cells was performed in 5-min intervals, under a wide-field fluorescence microscope. Cyan stars indicate nuclear translocation of NFAT after light illumination. Scale bar = 50 μm. EGFP, enhanced green fluorescent protein; NFAT, nuclear factor of activated T cell

activation of the NF-κB transcription factor (Figure 7). Therefore, we applied the NF-κB inhibitor, which significantly decreased the rate of cell migration (Figure 8). These results showed that Ca^{2+} affects cell migration by activating NF-κB (Liu et al., 2014). This finding also demonstrates that Ca^{2+} can increase the cell migration speed, when there is enough Ca^{2+} influx in the cells.

In addition to transcription factor activation, Ca^{2+} oscillations also affect certain cell migration-related signaling pathways (Aoki et al., 2007; Pauly et al., 1995; Xu et al., 2016). Western blot analysis analysis revealed that Ca^{2+} oscillations produced by 0.01 Hz frequency could activate ERK and AKT, but not Stat3, p38, or JNK (Figure S3). ERK was mainly activated from 30 min to 3 h of light treatment, whereas AKT was mainly activated from 15 min to 2 h of light treatment. Thus, the MEK1/2 inhibitor U0126 and PI3K inhibitors LY294002 and Wortmannin were used in subsequent experiments to examine the involvement of ERK and AKT. As shown in Figure S4, the MEK1/2 inhibitor U0126 inhibited cell migration at 24 h (Figure S4). In addition, the PI3K inhibitors LY294002 and Wortmannin exerted a similar inhibitory effect on Ca^{2+} oscillation-mediated increased cell migration (Figure S5). Finally, we used Western blot analysis to confirm the effectiveness of the inhibitors and found they significantly limited ERK and AKT activation (Figure S2). This suggests that whether activation of ERK and AKT contribute to Ca^{2+} oscillation-mediated cell migration is still inconclusive. It is possible that these drugs (U0126, LY294002 and Wortmannin) have other side effects in addition to ERK and AKT activation.

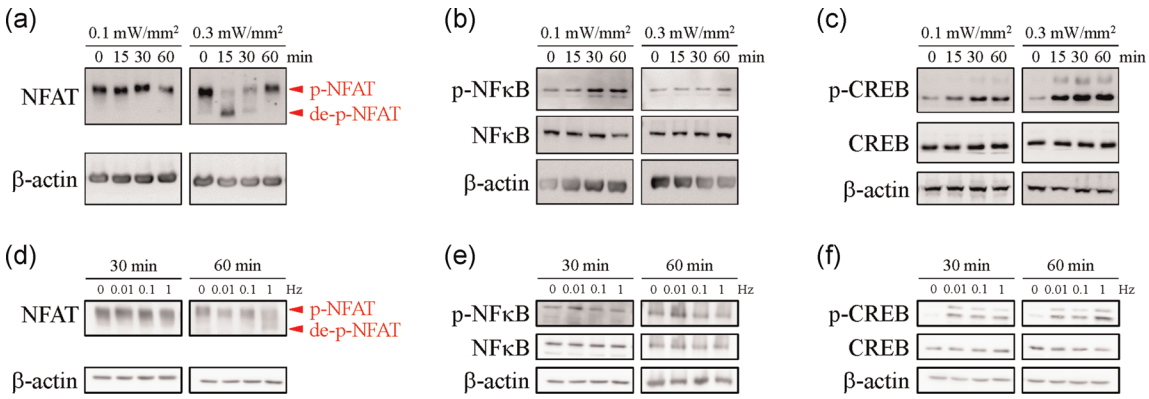

FIGURE 7 Differential activation of transcription factors depends on the modes of Ca^{2+} oscillations. NFAT, NF-κB, and CREB are the most important Ca^{2+}-dependent transcription factors. (a–c) U2OS cells overexpressing CatCh were illuminated at 0.1 mW/mm^2 or 0.3 mW/mm^2 intensity, 1 Hz frequency, and 500 ms duty cycle for 15, 30, and 60 min. (d–f) U2OS-CatCh cells after 30 or 60 min of illumination with light of different frequencies (0.01, 0.1, and 1 Hz) at 0.1 mW/mm^2 fixed power and 100 ms duty cycle. (a,d) NFAT, (b,e) phospho-NF-κB (p-NF-κB), NF-κB, (c,f) phospho-CREB (p-CREB), and CREB were detected using immunoblotting. β-actin served as the internal control. Arrowheads indicate phosphorylated NFAT (p-NFAT) and dephosphorylated NFAT (de-p-NFAT), respectively. CREB, cAMP response element binding protein; NFAT, nuclear factor of activated T cell; NF-κB, nuclear factor κ-light-chain-enhancer of activated B cell

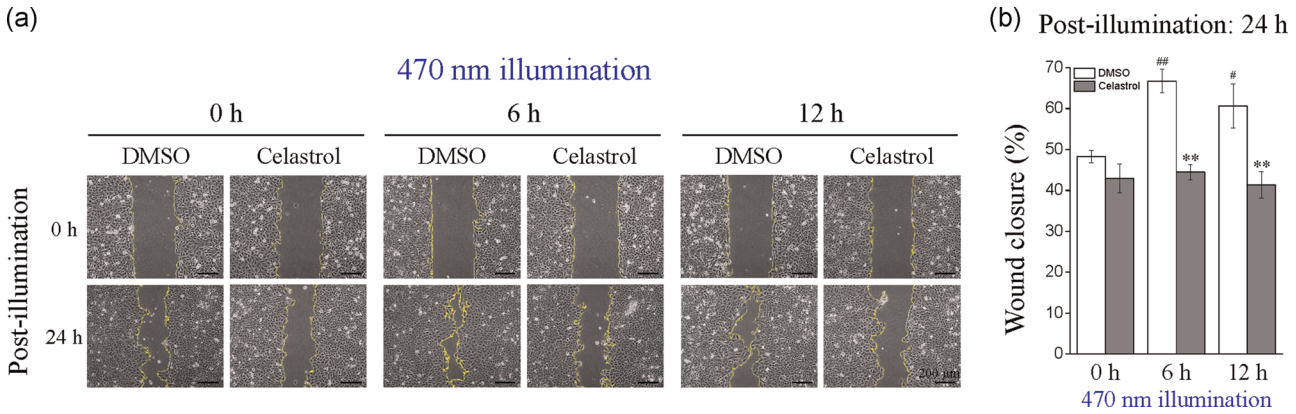

FIGURE 8 Inhibition of NF-κB decreases the migration of U2OS-CatCh cells upon blue light stimulation. The in vitro wound healing migration assay was performed to evaluate the effect of light illumination on cell migration. U2OS-CatCh cells were seeded into silicon inserts with 10% FBS medium. Following cell adhesion, inserts were removed, and the cells were cultured for 24 h. Phase images were captured at 0 and 24 h, and wound spaces were analyzed using ImageJ. (a) Cells were pretreatment with the NF-κB inhibitor (100 nM Celastrol) for 30 min before insert removal. After insert removal, U2OS-CatCh cells were illuminated with 470 nm blue light at 0.01 Hz, 0.1 mW/mm^2 intensity, 100 ms duty cycle, and 6 and 12 h duration. (b) Cell migration is presented as the percentage of wound closure. Each bar represents mean ± *SEM* from three independent experiments. ANOVA, analysis of variance; DMSO, dimethyl sulfoxide; FBS, fetal bovine serum; NF-κB, nuclear factor κ-light-chain-enhancer of activated B cell. #Significant difference between cells treated with or without light illuminations. *Significant difference between cells treated with or without Celastrol. $^{\#}p < .05$; $^{**,\#\#}p < .01$, calculated by one-way ANOVA

In this study, by using optogenetics, we have identified that the individual Ca^{2+} waves could activate cell migration via the activation of the Ca^{2+}-dependent transcription factor NF-κB. Thus, we can choose optical parameters (density, frequency, and duty cycle) to modulate Ca^{2+} waves and achieve activation of specific signaling pathways. This methodology can be applied to clarify related cell-signaling mechanisms in the future.

ACKNOWLEDGMENTS

We thank the Bio-image Core Facility of the National Core Facility Program for Biopharmaceuticals, Ministry of Science and Technology from Taiwan for their technical services. This study was supported by the Ministry of Science and Technology of Taiwan [MOST 109-2628-B-006-012 and MOST 109-2320-B-006-037].

CONFLICT OF INTERESTS

The authors declare that there are no conflict of interests.

AUTHOR CONTRIBUTIONS

Yi-Shyun Lai, Ya-Han Chang, and Wen-Tai Chiu designed the experiments. Yi-Shyun Lai, Ya-Han Chang, Yong-Yi Chen, Jixuan Xu and Chi-Sian Yu conducted the experiments; Yi-Shyun Lai and Ya-Han Chang participated in the data analysis. Su-Jing Chang, Pai-Sheng Chen, and Shaw-Jenq Tsai provided technical support. Yi-Shyun Lai and Wen-Tai Chiu drafted and polished the manuscript. All authors read and approved the final manuscript.

DATA AVAILABILITY STATEMENT

The data that support the findings of this study are available from the corresponding author upon reasonable request.

ORCID

Pai-Sheng Chen http://orcid.org/0000-0003-0513-1467
Shaw-Jenq Tsai http://orcid.org/0000-0002-3569-5813
Wen-Tai Chiu http://orcid.org/0000-0003-0310-0675

REFERENCES

Aoki, K., Kondo, Y., Naoki, H., Hiratsuka, T., Itoh, R. E., & Matsuda, M. (2007). Propagating wave of ERK activation orients collective cell migration. *Developmental Cell*, *43*(3), 305–317. https://doi.org/10.1016/j.devcel.2017.10.016

Bass, C. E., Grinevich, V. P., Vance, Z. B., Sullivan, R. P., Bonin, K. D., & Budygin, E. A. (2010). Optogenetic control of striatal dopamine release in rats. *Journal of Neurochemistry*, *114*(5), 1344–1352. https://doi.org/10.1111/j.1471-4159.2010.06850.x

Berchtold, M. W., & Villalobo, A. (2014). The many faces of calmodulin in cell proliferation, programmed cell death, autophagy, and cancer. *Biochimica et Biophysica Acta*, *1843*(2), 398–435. https://doi.org/10.1016/j.bbamcr.2013.10.021

Berridge, M. J., Bootman, M. D., & Lipp, P. (1998). Calcium—A life and death signal. *Nature*, *395*(6703), 645–648. https://doi.org/10.1038/27094

Berridge, M. J., Bootman, M. D., & Roderick, H. L. (2003). Calcium signalling: Dynamics, homeostasis and remodelling. *Nature Reviews Molecular Cell Biology*, *4*(7), 517–529. https://doi.org/10.1038/nrm1155

Berridge, M. J., Lipp, P., & Bootman, M. D. (2000). The versatility and universality of calcium signaling. *Nature Reviews Molecular Cell Biology*, *1*(1), 11–21. https://doi.org/10.1038/35036035

Boulware, M. J., & Marchant, J. S. (2008). Timing in cellular Ca^{2+} signaling. *Current Biology*, *18*(17), R769–R776. https://doi.org/10.1016/j.cub.2008.07.018

Chen, Y. F., Chen, Y. T., Chiu, W. T., & Shen, M. R. (2013). Remodeling of calcium signaling in tumor progression. *Journal of Biomedical Science*, *20*(1), 23. https://doi.org/10.1186/1423-0127-20-23

Colella, M., Grisan, F., Robert, V., Turner, J. D., Thomas, A. P., & Pozzan, T. (2008). Ca^{2+} oscillation frequency decoding in cardiac

cell hypertrophy: Role of calcineurin/NFAT as Ca^{2+} signal integrators. *Proceedings of the National Academy of Sciences of the United States of America*, *105*(8), 2859–2864. https://doi.org/10.1073/pnas.0712316105

Dedkova, E. N., Sigova, A. A., & Zinchenko, V. P. (2000). Mechanism of action of calcium ionophores on intact cells: Ionophore-resistant cells. *Membrane & Cell Biology*, *13*(3), 357–368.

Dolmetsch, R. E., Lewis, R. S., Goodnow, C. C., & Healy, J. I. (1997). Differential activation of transcription factors induced by Ca^{2+} response amplitude and duration. *Nature*, *386*(6627), 855–858. https://doi.org/10.1038/386855a0

Fenno, L., Yizhar, O., & Deisseroth, K. (2011). The development and application of optogenetics. *Annual Review of Neuroscience*, *34*, 389–412. https://doi.org/10.1146/annurev-neuro-061010-113817

Feske, S. (2007). Calcium signaling in lymphocyte activation and disease. *Nature Reviews Immunology*, *7*(9), 690–702. https://doi.org/10.1038/nri2152

Fiorio Pla, A., Kondratska, K., & Prevarskaya, N. (2016). STIM and ORAI proteins: Crucial roles in hallmarks of cancer. *American Journal of Physiology–Cell Physiology*, *310*(7), C509–C519. https://doi.org/10.1152/ajpcell.00364.2015

Franco, S. J., & Huttenlocher, A. (2005). Regulating cell migration: Calpains make the cut. *Journal of Cell Science*, *118*(Pt 17), 3829–3838. https://doi.org/10.1242/jcs.02562

Hajnoczky, G., Cordas, G., Madesh, M., & Pacher, P. (2000). Control of apoptosis by IP_3 and ryanodine receptor driven calcium signal. *Cell Calcium*, *28*(5–6), 349–363. https://doi.org/10.1054/ceca.2000.0169

Hannanta-Anan, P., & Chow, B. Y. (2016). Optogenetic control of calcium oscillation waveform defines NFAT as an integrator of calcium load. *Cell Systems*, *2*(4), 283–288. https://doi.org/10.1016/j.cels.2016.03.010

Huang, C., Jacobson, K., & Schaller, M. D. (2004). MAP kinases and cell migration. *Journal of Cell Science*, *117*(Pt 20), 4619–4628. https://doi.org/10.1242/jcs.01481

Huang, Y. W., Chang, S. J., Harn, H. I. C., Huang, H. T., Lin, H. H., Shen, M. R., Tang, M. J., & Chiu, W. T. (2015). Mechanosensitive store-operated calcium entry regulates the formation of cell polarity. *Journal of Cellular Physiology*, *230*(9), 2086–2097. https://doi.org/10.1002/jcp.24936

Huttenlocher, A., Palecek, S. P., Lu, Q., Zhang, W., Mellgren, R. L., Lauffenburger, D. A., Ginsberg, M. H., & Horwitz, A. F. (1997). Regulation of cell migration by the calcium-dependent protease calpain. *The Journal of Biological Chemistry*, *272*(52), 32719–32722. https://doi.org/10.1074/jbc.272.52.32719

Kar, P., Bakowski, D., Di Capite, J., Nelson, C., & Parekh, A. B. (2012). Different agonists recruit different stromal interaction molecule proteins to support cytoplasmic Ca^{2+} oscillations and gene expression. *Proceedings of the National Academy of Sciences of the United States of America*, *109*(18), 6969–6974. https://doi.org/10.1073/pnas.1201204109

Kass, G. E., & Orrenius, S. (1999). Calcium signaling and cytotoxicity. *Environmental Health Perspectives*, *107*(Suppl 1), 25–35. https://doi.org/10.1289/ehp.99107s125

Kim, J. M., Lee, M., Kim, N., & Heo, W. D. (2016). Optogenetic toolkit reveals the role of Ca^{2+} sparklets in coordinated cell migration. *Proceedings of the National Academy of Sciences of the United States of America*, *113*(21), 5952–5957. https://doi.org/10.1073/pnas.1518412113

Kleinlogel, S., Feldbauer, K., Dempski, R. E., Fotis, H., Wood, P. G., Bamann, C., & Bamberg, E. (2011). Ultra light-sensitive and fast neuronal activation with the Ca^{2+}-permeable channelrhodopsin CatCh. *Nature Neuroscience*, *14*(4), 513–518. https://doi.org/10.1038/nn.2776

Li, W., Llopis, J., Whitney, M., Zlokarnik, G., & Tsien, R. Y. (1998). Cell-permeant caged $InsP_3$ ester shows that Ca^{2+} spike frequency can optimize gene expression. *Nature*, *392*(6679), 936–941. https://doi.org/10.1038/31965

Liu, J., Liu, Q., Wan, Y., Zhao, Z., Yu, H., Luo, H., & Tang, Z. (2014). Osteopontin promotes the progression of gastric cancer through the NF-κB pathway regulated by the MAPK and PI3K. *International Journal of Oncology*, *45*(1), 282–290. https://doi.org/10.3892/ijo.2014.2393

Mascia, F., Denning, M., Kopan, R., & Yuspa, S. H. (2012). The black box illuminated: Signals and signaling. *The Journal of Investigative Dermatology*, *132*(3 Pt 2), 811–819. https://doi.org/10.1038/jid.2011.406

Mei, Y., & Zhang, F. (2012). Molecular tools and approaches for optogenetics. *Biological Psychiatry*, *71*(12), 1033–1038. https://doi.org/10.1016/j.biopsych.2012.02.019

Nagel, G., Ollig, D., Fuhrmann, M., Kateriya, S., Musti, A. M., Bamberg, E., & Hegemann, P. (2002). Channelrhodopsin-1: A light-gated protein channel in green algae. *Science*, *296*(5577), 2395–2398. https://doi.org/10.1126/science.1072068

Nagel, G., Szellas, T., Huhn, W., Kateriya, S., Adeishvili, N., Berthold, P., Ollig, D., Hegemann, P., & Bamberg, E. (2003). Channelrhodopsin-2, a directly light-gated cation-selective membrane channel. *Proceedings of the National Academy of Sciences of the United States of America*, *100*(24), 13940–13945. https://doi.org/10.1073/pnas.1936192100

Nankova, B., Hiremagalur, B., Menezes, A., Zeman, R., & Sabban, E. (1996). Promoter elements and second messenger pathways involved in transcriptional activation of tyrosine hydroxylase by ionomycin. *Brain Research. Molecular Brain Research*, *35*(1-2), 164–172. https://doi.org/10.1016/0169-328x(95)00201-3

Ong, H. L., Jang, S. I., & Ambudkar, I. S. (2012). Distinct contributions of Orai1 and TRPC1 to agonist-induced $[Ca^{2+}]_i$ signals determine specificity of Ca^{2+}-dependent gene expression. *PLoS One*, *7*(10), e47146. https://doi.org/10.1371/journal.pone.0047146

Parekh, A. B. (2011). Decoding cytosolic Ca^{2+} oscillations. *Trends in Biochemical Sciences*, *36*(2), 78–87. https://doi.org/10.1016/j.tibs.2010.07.013

Pauly, R. R., Bilato, C., Sollott, S. J., Monticone, R., Kelly, P. T., Lakatta, E. G., & Crow, M. T. (1995). Role of calcium/calmodulin-dependent protein kinase II in the regulation of vascular smooth muscle cell migration. *Circulation*, *91*(4), 1107–1115. https://doi.org/10.1161/01.cir.91.4.1107

Ridley, A. J., Schwartz, M. A., Burridge, K., Firtel, R. A., Ginsberg, M. H., Borisy, G., … Horwitz, A. R. (2003). Cell migration: Integrating signals from front to back. *Science*, *302*(5651), 1704–1709. https://doi.org/10.1126/science.1092053

Smedler, E., & Uhlén, P. (2014). Frequency decoding of calcium oscillations. *Biochimica et Biophysica Acta*, *1840*(3), 964–969.

Song, S., Li, J., Zhu, L., Cai, L., Xu, Q., Ling, C., Su, Y., & Hu, Q. (2012). Irregular Ca^{2+} oscillations regulate transcription via cumulative spike duration and spike amplitude. *The Journal of Biological Chemistry*, *287*(48), 40246–40255. https://doi.org/10.1016/j.bbagen.2013.11.015

Sun, S., Liu, Y., Lipsky, S., & Cho, M. (2007). Physical manipulation of calcium oscillations facilitates osteodifferentiation of human mesenchymal stem cells. *FASEB Journal*, *21*(7), 1472–1480. https://doi.org/10.1096/fj.06-7153com

Sáez, P. J., Villalobos-Labra, R., Westermeierm, F., Sobrevia, L., & Farías-Jofré, M. (2014). Modulation of endothelial cell migration by ER stress and insulin resistance: A role during maternal obesity? *Frontiers in Pharmacology*, *5*, 189. https://doi.org/10.3389/fphar.2014.00189

Tsai, H. C., Zhang, F., Adamantidis, A., Stuber, G. D., Bonci, A., de Lecea, L., & Deisseroth, K. (2009). Phasic firing in dopaminergic neurons is sufficient for behavioral conditioning. *Science*, *324*(5930), 1080–1084. https://doi.org/10.1126/science.1168878

Uhlén, P., & Fritz, N. (2010). Biochemistry of calcium oscillations. *Biochemical and Biophysical Research Communications*, *396*(1), 28–32. https://doi.org/10.1016/j.bbrc.2010.02.117

Wei, C., Wang, X., Chen, M., Ouyang, K., Song, L. S., & Cheng, H. (2009). Calcium flickers steer cell migration. *Nature*, *457*(7231), 901–905. https://doi.org/10.1038/nature07577

Wei, C., Wang, X., Zheng, M., & Cheng, H. (2012). Calcium gradients underlying cell migration. *Current Opinion in Cell Biology*, *24*(2), 254–261. https://doi.org/10.1016/j.ceb.2011.12.002

Whitaker, M. (2006). Calcium at fertilization and in early development. *Physiological Reviews*, *86*(1), 25–88. https://doi.org/10.1152/physrev.00023.2005

Xie, J., Pan, H., Yao, J., Zhou, Y., & Han, W. (2016). SOCE and cancer: Recent progress and new perspectives. *International Journal of Cancer*, *138*(9), 2067–2077. https://doi.org/10.1002/ijc.29840

Xu, Y., Nan, D., Fan, J., Bogan, J. S., & Toomre, D. (2016). Optogenetic activation reveals distinct roles of PIP_3 and Akt in adipocyte insulin action. *Journal of Cell Science*, *129*(10), 2085–2095. https://doi.org/10.1242/jcs.174805

SUPPORTING INFORMATION

Additional Supporting Information may be found online in the supporting information tab for this article.

How to cite this article: Lai Y-S, Chang Y-H, Chen Y-Y, et al. Ca^{2+}-regulated cell migration revealed by optogenetically engineered Ca^{2+} oscillations. *J Cell Physiol*. 2021;236:4681–4693. https://doi.org/10.1002/jcp.30190